Macromolecules

Article

Interplay between Viscoelasticity and Force Rate Affects Sequential Unfolding in Polyproteins Pulled at Constant Velocity

Moran Elias-Mordechai, Einat Chetrit, and Ronen Berkovich*

Read Online

ACCESS | Metrics & More | Article Recommendations | SI Supporting Information

ABSTRACT: Polyproteins are unique constructs, comprised of folded protein domains in tandem and polymeric linkers. These macromolecules perform under biological stresses by modulating their response through partial unfolding and extending. Although these unfolding events are considered independent, a history dependence of forced unfolding within polyproteins was reported. Here we measure the unfolding of single poly(I91) octamers, complemented with Brownian dynamics simulations, displaying increasing hierarchy in unfolding-foces, accompanied by a decrease in the effective stiffness. This counters the existing understanding that relates stiffness with variations in domain size and probe stiffness, which is expected to reduce the unfolding forces with every consecutive unfolding event. We utilize a simple mechanistic viscoelastic model to show that two effects are combined within a sequential forced unfolding process: the viscoelastic properties of the growing linker chain lead to a hierarchy of the unfolding events, and force-rate application governs the unfolding kinetics.
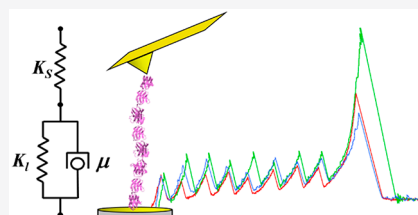
INTRODUCTION

Polyproteins are biological constructs made of proteins repeats tethered in tandem, often related to physiological activity that involves mechanical stresses, such as muscle contractions,[1,2] mechano-transduction,[3,4] etc. Their unique structure enables them to respond to the applied load by unfolding some of their folded domains and extend them in order to regulate stresses and energy,[1,2] adjust cell adhesion,[5,6] reveal hidden sites,[3,7] and enable actin cross-linking.[8] The mechanical response of polyproteins to external forces has been extensively studied using single-molecule force spectroscopy (SMFS) through conformational changes, such as unfolding, folding and collapse, in response to various forms of direct load application protocols.[9−20] In force extension (FX) measurements, direct load is applied to a single polyprotein molecule, which is tethered at both termini, by pulling it at constant velocity. As a result, the polyprotein displays a series unfolding events in a characteristic "sawtooth" pattern, where each unfolding event occurs at a specific maximal force. Each unfolding event is followed by rapid relaxation due to the exposed length of the unfolded domain, which then is extended due to the continuous application of external load until the next domain unfold and *vice versa*.

SMFS approach relays on a device to which the molecule of interest (RNA hairpins/proteins/polyproteins) under investigation is tethered (cantilevers tips/beads), and a polymeric linker (connecting amino acid sequences/unfolded domains polypeptides/folded domains). Thereby, a growing body of literature studies the effects introduced by the application of force to the recorded unfolding/rupture probabilities and rates.[11,18,20−40] Specifically to polyprotein constructs, sequential hierarchy in the measured unfolding forces was reported

using FX SMFS studies of I91 polyproteins.[11,37,41,42] This unfolding history dependency was explained as a biphasic behavior, resulting from two competing effects: (a) increase of domain unfolding probability with each unfolding event along the polyprotein chain (N-effect), and (b) decrease of domain unfolding rates resulting from an increase in the cantilever-polymeric (linker) component of the polyprotein after each unfolding event (compliance effect). According to the latter, with the consecutive unfolding of each domain, the overall compliance (inverse of the chain effective stiffness) grows. It is claimed that while the first (N) effect tends to increase the force required to unfold domains with the reduction of the number of folded domains, the second (stiffness) effect inclines to reduce the unfolding forces along the elongating unfolded chain with the increase of the cantilever spring constants. Numerical Monte Carlo simulations exemplified the biphasic behavior for considerably large domains, and increasing number of domains and cantilever spring constants.[11] Other works also demonstrated that the unfolding forces depend not only on the pulling velocity but also on the stiffness of the pulling device.[32,38] A recent study on the history of mechanical unfolding of I91 polyprotein showed a monotonous increase of the unfolding forces in time (with no biphasic behavior),[18] which was explained by the use of
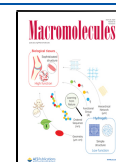
long linkers that eliminate possible nonspecific interaction of the first unfolding domain with the surface.

Here we suggest that sequential unfolding in a polyprotein results from an interplay between the viscoelastic properties of its elongating polymeric linker after each unfolding event[12,43] and the direct effect of the applied force-rate, dF/dt on the unfolding probabilities.[44−46] This interplay eventually encapsulates the two effects mentioned above (compliance and event probability[11,37]) as a manifestation of the same phenomenon. The application of higher loading rates, with the increase in the pulling velocity, is associated with the reduction of the unfolded chain internal friction, which propagates the tension faster through the stretched elongating linker. Accordingly, the effect of the applied mechanical work on the polyprotein domains becomes more direct. While previous works focused on the stiffness of the pulling device and the nonlinear elasticity of the polymeric linkers on the unfolding probabilities, this work investigates the relation between the variations in the local stiffness of the polyprotein (linker and folded/unfolded domains) and internal friction of the elongating linker at high extensions and their relation to hierarchical unfolding forces within a polyprotein under tension. To this end we performed FX SMFS measurements using atomic force microscopy (AFM) on octameric repeats of I91 domain, denoted as poly(I91), pulled at a constant velocity, V [nm/s]. We use a simple mechanistic viscoelastic model to describe the dynamical response of the molecule−-probe system in order to explain the observed behavior. The experiments were complemented with Brownian dynamics (BD) simulations that reproduced the experimentally observed trend, where the mean unfolding forces corresponds to domain number, in concert with the changes in the chain viscoelastic properties and local unfolding rates.

EXPERIMENTAL SECTION

Materials. Poly(I91) octamers were expressed and purified in the laboratory of Dr. Neta Sal-Man at Ben-Gurion University of the Negev, using plasmids that were kindly provided by Prof. J. M. Fernandez from Columbia University. The proteins were purified using HEPES buffer (1.0 mM EDTA, 150 mM NaCl, 20 mM HEPES, pH 7.5) as described elsewhere.[47]

Atomic Force Spectroscopy Measurements. Pulling experiments were carried out with a Luigs & Neumann LTD AFM. The polyprotein solution was centrifuged at 14 000 rpm at 4 °C for 4 min. Next, 20 μL of polyprotein solution was deposited on gold-coated glass coverslides. The glass coverslides were rinsed with 99.9% ethanol (Romical) followed by deionized water (Ultra 370 series, Aqua Max, 18.2 MΩ·cm), then coated with Ni layer and topped with an Au layer by thermal evaporation (Quorum K975X) at 14 mA and 3 min for each layer. All the measurements were carried out in ambient conditions at room temperature. The force-extension (FX) measurements were performed on piezo movement velocities ranging between 50 and 1000 nm/s. The traces were fitted with the Worm-Like-Chain model[48,49] to properly identify the I91 domains, resulting with a mean persistence length $\langle l_p \rangle$ = 0.4 ± 0.1 nm and mean contour length increment $\langle \Delta L_C \rangle$ = 27.6 ± 0.5 nm. Since the polyprotein attach to the cantilever at random position, traces that were collected had 6−8 unfolding events in the measurements. The cantilevers used (gold-coated Si-Ni Biolevers, BL-TR400PB Asylum Research, Oxford Instruments) were calibrated prior to each experiment using the equipartition theorem,[50] measuring spring constants, K_S, ranging between 24 and 26 pN/nm. The measurements were carried out in HEPES buffer. Data analysis was performed using IGOR Pro 6.3.7.2 software (WaveMetrics) and Matlab (R2013b).

Brownian Dynamics Simulations. The dynamics of a polyprotein unfolding under constant velocity were numerically

reproduced by integrating a set of nine conjugated overdamped Langevin equations[29] using Matlab (R2013b). Full details are provided in the Supporting Information (SI).

RESULTS AND DISCUSSION

We measured the unfolding dynamics by pulling on an eight domain poly(I91) at several velocities varying from 50 to 1000 nm/s. Accordingly, N (= 1−8) unfolding events were observed in the sawtooth curve.[9,15] Since no specific attachment technique was implemented (to avoid the effect of an additional long linker), each polyprotein molecule can be arbitrary picked up by the cantilever tip at any domain between the first one to the eighth. Consequently, we excluded unfolding traces that displayed less than five events, which provided the following average number of data points for the analysis of the unfolding events: n = 65 for the first through fifth events, 50 for the sixth, 31 for the seventh, and 8 for the eighth. Since the recorded number of traces with eight unfolded events were too low to estimate reliable statistics (ranging from 1 to 12, with an average of 8), we relate in the analyses to the unfolding events in the polyprotein up to the seventh event.

Figure 1A shows three representative FX traces with eight unfolding events, measured at V = 50, 100, and 1000 nm/s (red, blue, and green, respectively). For simplicity, in the following we will present the analysis for these three velocities with their color coding, and compare the observed trends to the ones obtained via BD simulations at three representative velocities of 40, 400, and 4000 nm/s. It can be clearly seen that the unfolding forces generally grow with the pulling velocity.[9,10,16,51] We examined the behavior of the unfolding forces (F_{max}) and stiffness for the each event at the various pulling velocities. The mean unfolding forces, calculated from the distributions of the maximal values collected from every unfolding peak, show a hierarchical increase with event number for all velocities, with no evidence of biphasic behavior. The same trend was observed in the forces obtained from the BD simulations at all velocities (see SI).

The overall effective stiffness can be estimated by taking the slope of the force with respect to its extension at the linear regime at high stretches, before the unfolding event. This effective stiffness encompasses contributions from the polyprotein components and the stiffness of the cantilever to which it is tethered according to

$$\left. \frac{dF}{dx}(N) \right|_{exp} = K_{eff}(N) = \left[\frac{1}{K_S} + \frac{1}{K_l(N)} + \frac{1}{K_P(N)} \right]^{-1}$$

(1)

where K_S is the spring constant of the cantilever, $K_l(N)$ is the stiffness of the polymeric linker after each unfolding event, and $K_P(N) = \sum K_{P,i}$, $i = 1−N$, are the stiffnesses of the remaining folded protein domains. The stiffness of the polymeric linkers can be approximated with an asymptotic phenomenological expression, based on the Worm-Like-Chain (WLC) model at high stretches:[43]

$$K_l(N) = \frac{4}{L_C(N)} \sqrt{\frac{l_p}{k_B T}} \{F[L_C(N)]\}^{3/2}$$

(2)

where the overall contour length is estimated at high stretch $x/L_C \approx 0.85$ by $L_C(N) \triangleq (8 - N + 1) \cdot L_{C,folded} + 0.85 \cdot (L_{C,0} + N \cdot L_{C,unfolded})$, with $L_{C,0}$ being the contour length of the initial
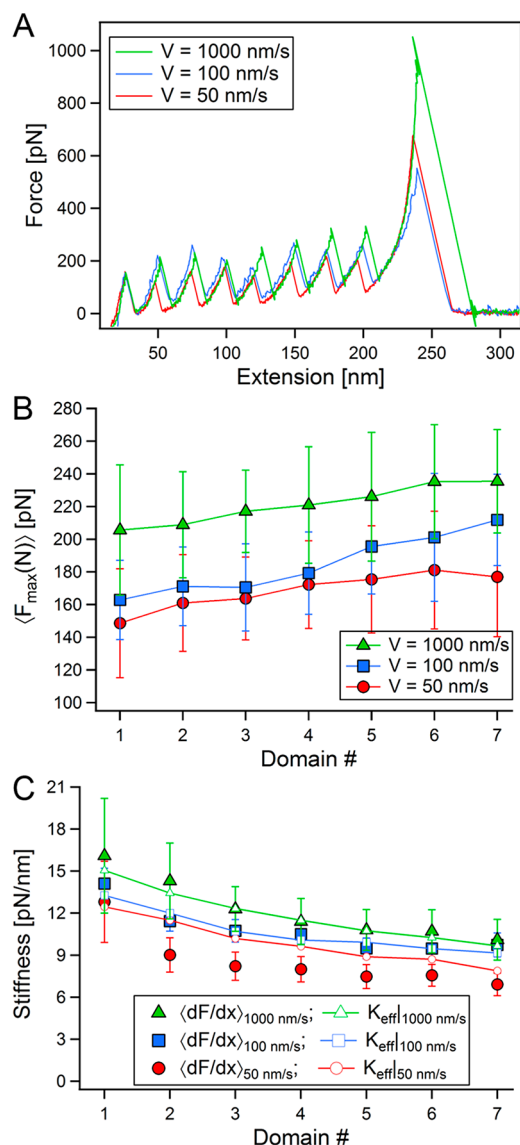
Figure 1. FX measurements of poly(I91) unfolding at three representative pulling velocities, V = 50 (red), 100 (blue), and 1000 (green) nm/s. (A) Three exemplary FX unfolding traces. (B) Mean unfolding forces (obtained from the maximal forces at each unfolding event) as a function of unfolding event (domain) number, N. (C) Mean chain stiffness, measured by the slope of the linear regime prior to each unfolding event (dF/dx), at each unfolding event (filled symbols), and the effective stiffness (K_{eff}), estimated with eq 2 and eq 3 (open symbols), showing a softening of the chain with the increase of its polymeric (linker) element after each unfolding event.

extension of the chain. The stiffness of a folded domain can be approximated by the second derivative of a Morse potential representing a one-dimensional projection of a protein energy landscape, $K_P = \nabla^2 U_P \approx 6(b/R_C)^2 U_0$,[52] with b being the curvature of the potential, R_C the size of an unfolded domain, and U_0 the unfolding barrier amplitude. Based on the characteristic values used for the BD simulations (see SI), the characteristic stiffness of a folded domain can be estimated as $K_P \approx 6210$ pN/nm, while the stiffness of the linker (unfolded domains) varies from $K_{l,n=1}|_{F\approx200\ pN} \approx 101$ pN/nm to $K_{l,n=8}|_{F\approx200\ pN} \approx 17$ pN/nm, which is in the same order of magnitude as K_S. Since a folded protein domain is much stiffer than the linker,[36] its contribution can thus be neglected

compared to those of the considerably more compliant linkers, and the overall effective stiffness can be written as (effective stiffness approximation[53])

$$K_{eff}(N, F) \cong \left[\frac{1}{K_S} + \frac{1}{K_l(N, F)}\right]^{-1} \tag{3}$$

Figure 1C plots the variation of stiffness of the system with domain number, comparing the mean of the measured slopes, $\langle dF/dx \rangle$, with K_{eff} calculated with eqs 3 and 2, using the corresponding experimental parameters. The stiffness shows a decrease with the progression of unfolding events. This result is not surprising, and was shown for a five repeat I91 polyprotein.[12] Additionally, stretched polymers were also shown to be effectively more flexible (reduce) under tension.[54] eq 3 predicts this behavior, as can be seen in Figure 1C, since according to it the stiffness of the linker is proportional to the inverse of its contour length, i.e., $K_{eff} \sim 1/L_C$. On the other hand, the stiffness is also expected to grow with the unfolding force ($K_{eff} \sim F^{3/2}$), which grows with N; however the observed increase in the unfolding forces (Figures 1B and S1B) is considerably milder compared to the increase in the extension of the polyprotein after each unfolding event, meaning that the increase in L_C has more prominent effect of the stiffness.

Within the distribution range, K_{eff} deviates from the measured $\langle dF/dx \rangle$, while still following the same general decreasing trend with N. This deviation is also apparent in the BD simulations (see SI). At low pulling velocities, K_{eff} overestimates $\langle dF/dx \rangle$, while at the other extreme (at high velocity) it lags behind it. Since the force vary nonlinearly as the chain elongates at constant pulling velocity, we estimated the local unfolding force-rates, dF/dt, at each unfolding event. The force-rate is typically estimated as the product of the velocity with the stiffness of the last unfolding event, i.e., $dF/dx|_{last\ event} \times V$. In addition to this approach, we evaluated force-rates by taking the slope of the maximal unfolding forces with respect to the times in which they occurred. Figure 2A shows the unfolding forces vs their event time measured at $V = 1000$ nm/s (triangles in green shades), with linear fittings (straight lines). Similar estimations were performed for the forces measured at the other lower pulling velocities, all displaying a similar decreasing of the force rates experienced by the polyproteins with unfolding progression.

Figure 2B plots the mean unfolding rates per sequential unfolding events at $V = 50$, 100, and 1000 nm/s (filled symbols), together with the local rates, estimated by $\langle dF/dx \rangle_N \times V$ (small open symbols). Both unfolding rates, estimated by the two approaches, decrease with the elongation of the linker, as N increases. Two important observables should be pointed. First, since the various domains along the polyprotein chain unfold at different rates, their mean would better describe the unfolding rate at a given pulling velocity than the one estimated by the final unfolding events, which have the lowest value (i.e., with $\langle dF/dx \rangle_N \times V$, rather than $dF/dx|_{last\ event} \times V$). Second, estimation of the unfolding rate with $\langle dF/dx \rangle \times V$ (or $K_{eff} \times V$) appear to considerably deviate from the direct dF/dt approach (the rates in Figure 2B are plotted on a logarithmic scale). The BD simulations resulted with similar behavior. Figure 2C shows the evaluation of dF/dt from the simulated data obtained at $V = 4000$ nm/s (triangles in gray shades), with linear fits (straight lines), and Figure 4D plots the measured unfolding rates (colored empty symbols) and the rates estimated by $\langle dF/dx \rangle_N \times V$ (solid symbols, line
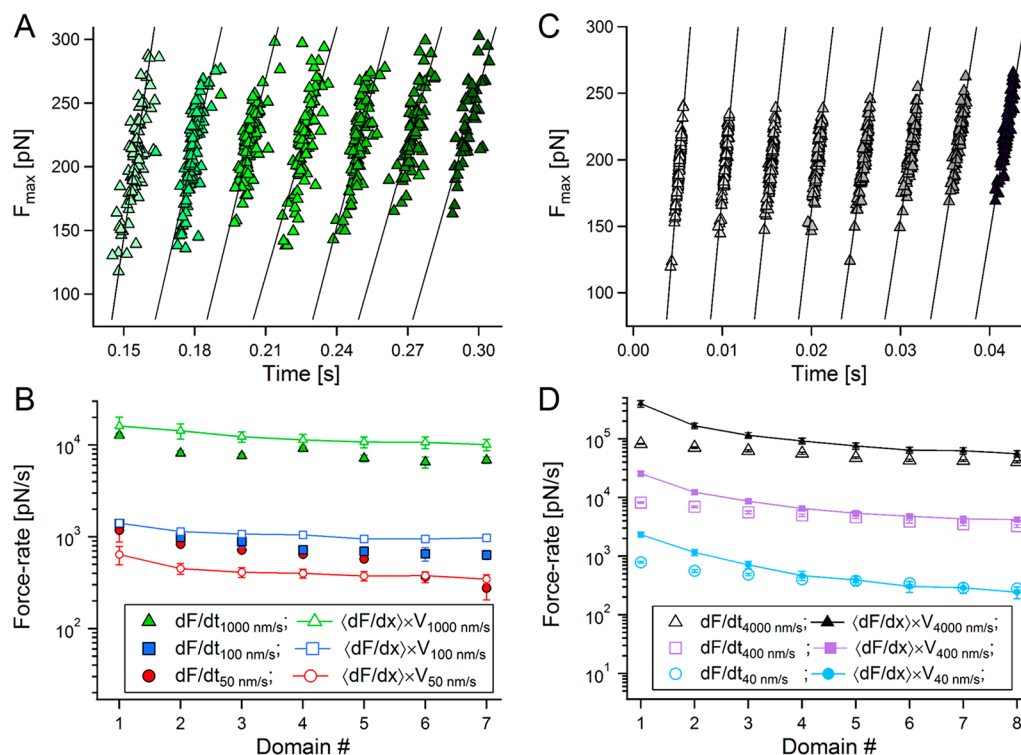
Figure 2. Force-rate variations with the domain number. (A) Unfolding forces (maximal forces, F_{max}, collected from the FX unfolding traces measured at $V = 1000$ nm/s) plotted against the time they took place on (green triangles, with increasing shade for each consecutive unfolding event). The slopes of the linear fits (solid black lines) estimate the local, event dependent, unfolding rate, dF/dt. (B) Force-rates from experimental data measured at $V = 50$ (red), 100 (blue), and 1000 (green) nm/s. dF/dt obtained from the slopes of the maximal unfolding forces with time (as in A) are marked by solid symbols, while rates estimated by $\langle dF/dx\rangle_N \times V$ are marked by blank, line connected small symbols. (C) Estimation of dF/dt from the maximal unfolding forces from BD simulations at $V = 4000$ nm/s. (D) Force-rates calculated from BD simulations at $V = 40$ (light blue), 400 (purple), and 4000 (black) nm/s.

connected small symbols) as a function of the increments in chain length (at the sequential unfolding of each domain).

The experimental data is naturally more scattered compared to the simulated data; however, both show similar trends. Due to the fact that the simulations benefit from larger statistics (100 data points per each events), without being subjected to experimental limitations (as it is only based on phenomenological models), it is consequently less noisy, and assists in providing a distilled picture of the experiments. Figure 2B shows that apart from $V = 50$ nm/s, at the other (higher) velocities the rate assessed by the stiffness ($\langle dF/dx\rangle_N \times V$) overestimates the values evaluated by dF/dt. This behavior is not observed in the simulated data (Figure 2D), where $\langle dF/dx\rangle_N \times V > (dF/dt)_N$. Figure 3A,B plots the N-averaged force-rates as a function of the applied pulling velocity for the experimental and the simulated data. As can be seen for both cases, apart from the experimental data at $V = 50$ nm/s, $\langle\langle dF/dx\rangle\rangle \times V > \langle dF/dt\rangle$. This exception probably results from the relatively large drift encountered when measuring at low velocities.

The varying polyprotein stiffness was observed (and predicted) to decrease with chain increase after every unfolding event; however, as can be seen in Figure 1C, it grows with the pulling velocity on average for each event. Figure 3C plots the N-averaged stiffness obtained from both experiments (tangerine triangles) and simulations (open triangles). The experimentally measured stiffness slightly increase, and shortly reaches a plateau, while the simulated stiffness seems to grow with the applied pulling velocity. This

indicates that the response of the polyprotein during unfolding under force is not purely elastic.

The modulation of the stiffness with the applied pulling velocity, raises questions regarding the nature and role of the polymeric linker that grows after every unfolding event along the polyprotein. The change of the stiffness with the velocity cannot be explained by eq 3, which disregards the viscoelastic nature of the extended linker, reflected through its internal friction, μ.[12,43] We therefore utilize the Zener model,[55] a constitutive model also known as the standard linear solid, which provides a useful idealized description of a viscoelastic material. It is described by a spring added in series to a Kelvin−Voigt model (spring and a dashpot in parallel), as depicted in Figure 4A. Equilibrium requires that the stress be the same in both elements, which can be indicated by estimating a critical velocity, $V_C \approx L_C(N)/\tau_{Zimm}$, below which, the extension of the chain can be considered to be in equilibrium.[56] $\tau_{Zimm} \approx 2^3(L_C l_p)^{3/2}\eta/[k_B T(3\pi)^{1/2}]$,[57] is the Zimm relaxation time for polymer chain (taking into account hydrodynamic interactions between its monomers[58]), where $\eta \approx 1 \times 10^{-3}$ Pa·s is the solvent viscosity. For the parameters obtained from our measurements $\langle V_C\rangle|_n \approx 1 \times 10^9$ nm/s, which are 8−6 orders of magnitude larger than the pulling velocities applied in our measurements, and therefore linker extension can be considered as an equilibrium process (unlike domain unfolding). In the context of this work, the linker is described by a stiffness K_l, given by eq 2, and a viscous term, μ, accounting for its internal friction in series with the spring constant of the probe, K_S:
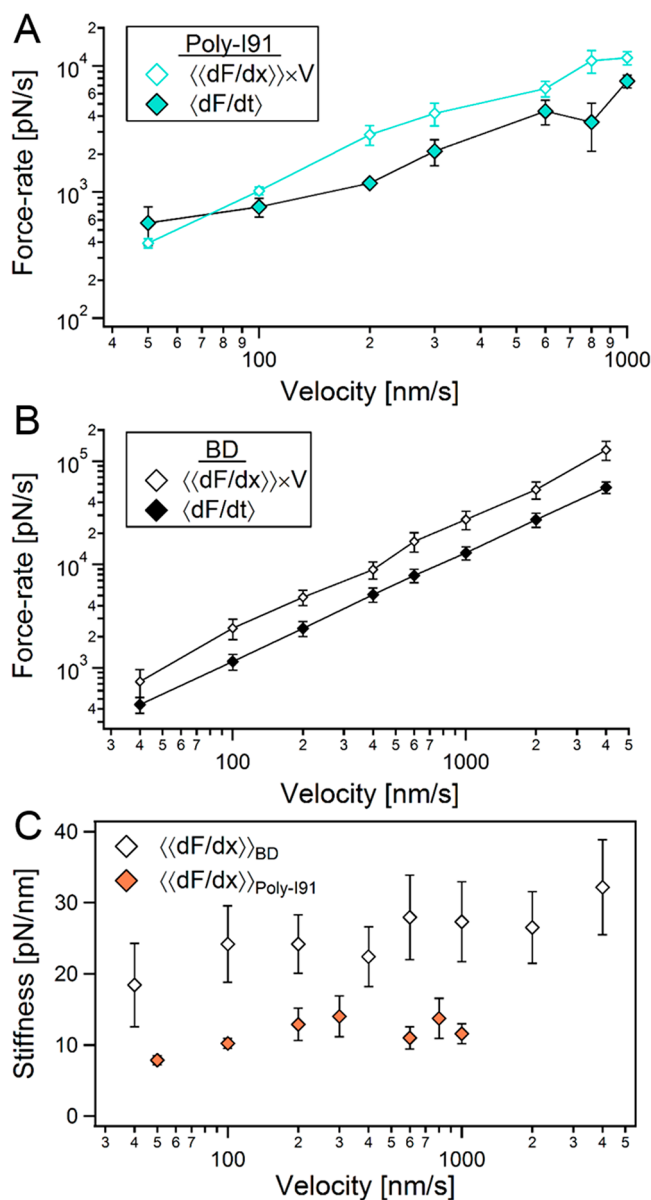
Figure 3. Effect of the pulling velocity on force-rates and chain stiffness. (A) Poly(I91) N-averaged force-rates $\langle dF/dt \rangle$ (solid turquoise diamonds) and $\langle\langle dF/dx \rangle\rangle \times V$ (small open turquoise diamonds) as a function of the pulling velocity. (B) BD N-averaged force-rates $\langle dF/dt \rangle$ (solid black diamonds) and $\langle\langle dF/dx \rangle\rangle \times V$ (small open diamonds) as a function of the pulling velocity. (C) N-averaged stiffness, $\langle\langle dF/dx \rangle\rangle$, as a function of the pulling velocity for poly(I91) (solid tangerine diamonds), and BD simulations (open diamonds).

$$F + \left(\frac{\mu}{K_S + K_l} \right) \frac{dF}{dt} = \left(\frac{K_S K_l}{K_S + K_l} \right) x + \left(\frac{K_S \mu}{K_S + K_l} \right) V \quad (4)$$

where the extension x can be approximated as L_C under the high stretch assumption.[43] Notice that the first term in the right-hand-side is K_{eff}, given by eq 3. When $dF/dt = K_S \cdot V$ (which is not the case here, as can be seen in Figures 2 and 3), then eq 4 reduces to the simple harmonic description, $F = K_{eff} \cdot x$, which means that the force dependency is purely elastic, and thus should not vary with the pulling velocity. Substituting eq 2 into this model and taking the derivative with respect to x, a connection can be established between dF/dx and μ (see SI for details):

$$\mu = \frac{\left[\frac{L_C(K_S + K_l)^2}{K_l} \right] \frac{\partial F}{\partial x} - L_C K_S K_l}{K_S V - \frac{\partial F}{\partial t}} \quad (5)$$

where $K_l = K_l(N, F)$ is given by eq 2, and $\partial F/\partial x \approx \langle dF/dx \rangle$. For a situation in which $dF/dt \ll K_S \cdot V$, μ diminishes, while at the opposite limit, where $dF/dt \rightarrow K_S \cdot V$, it becomes more dominant. Using the experimental parameters, we used eq 5 to calculate μ. Figure 4B,C shows that μ decreases with the extension of the chain length and with the applied velocity, respectively. Figure 4D,E shows the equivalent behavior of μ calculated from BD simulations. The decrease of μ with the increase in chain length is not so obvious from the experimental data, showing almost no change, and even a slight increase. μ calculated from the simulated data with eq 5, however, displays an explicit decrease with the increase in chain length, in agreement with previous works.[12,43] The decrease of μ with the length of the linker can be understood in terms of its proximity to the surface, which can be represented with Faxén correction for the hydrodynamic drag parallel to the direction of the force application (up to the second order) by[59] $\mu(x) \approx \mu_0/[1 - 9/16(a_{eff}/x)]$, with $\mu_0 = 6\pi\eta a_{eff}$, where η is the solution viscosity and a_{eff} is an effective size of the cantilever tip.[25] According to this description, the friction decrease to a characteristic μ_0 at sufficient distance from the surface.

The observed decrease of μ with V can also be expected (as the decrease of the stiffness with the extension). The force acting on the linker, represented here by a Kelvin−Voigt circuit is $F = K_l \cdot x + \mu \cdot V$. This expression states that μ is proportional to the inverse of V (and the stiffness is proportional to the inverse of x). Remarkably, Lee and Thirumalai introduced an expression for velocity dependent force, with a general form analogues to the Kelvin−Voigt circuit for long DNA molecules, where $K_l \equiv k_B T/(L_C \cdot l_p)$ is the stiffness of a Gaussian chain, and $\mu \equiv \mu_0 \cdot g(x)$, with $\mu_0 = k_B T/D_0$, where D_0 is the monomeric diffusion constant and $g(x) = (1/8) \cdot (x/L_C)^2/[1 - (x/L_C)^2]\}$ is a geometric factor on which the effective friction depends.[56]

According to the viscoelastic description of the linker, it is possible to understand the stiffening of the linker with the applied velocity, as μ decreases with the overall stiffness. This occurs with the increase of the pulling velocity, resulting in high force-rates (see SI). This behavior coexists with the increase in the internal friction with the chain stiffness as the chain becomes shorter; i.e., for a chain with increasing length, both stiffness and internal friction decrease under similar loads. We therefore turn to examine these effects on the recorded unfolding forces during the sequential unfolding within a polyprotein. As unfolding progresses, the elongating polymeric linker becomes more compliant as its stiffness decreases (Figure 1C) for a given pulling velocity (V = const.); however, an increase in the unfolding forces is observed (Figure 1B). This observable is shown in Figure 5A, where unfolding forces lessen with the increase of the overall stiffness of the system. Since the poly(I91) used here are homopolyproteins, it is a reasonable assumption that their protein domains are nearly similar, and can therefore be characterized by a relatively narrow distribution of unfolding barriers. The measured restoring forces during unfolding, $\langle F_{max} \rangle$ are proportional to the stress required to overcome a characteristic energy activation barrier, $\langle U_0 \rangle$ (with a variance that results from thermal fluctuations and possible structural variations). In the
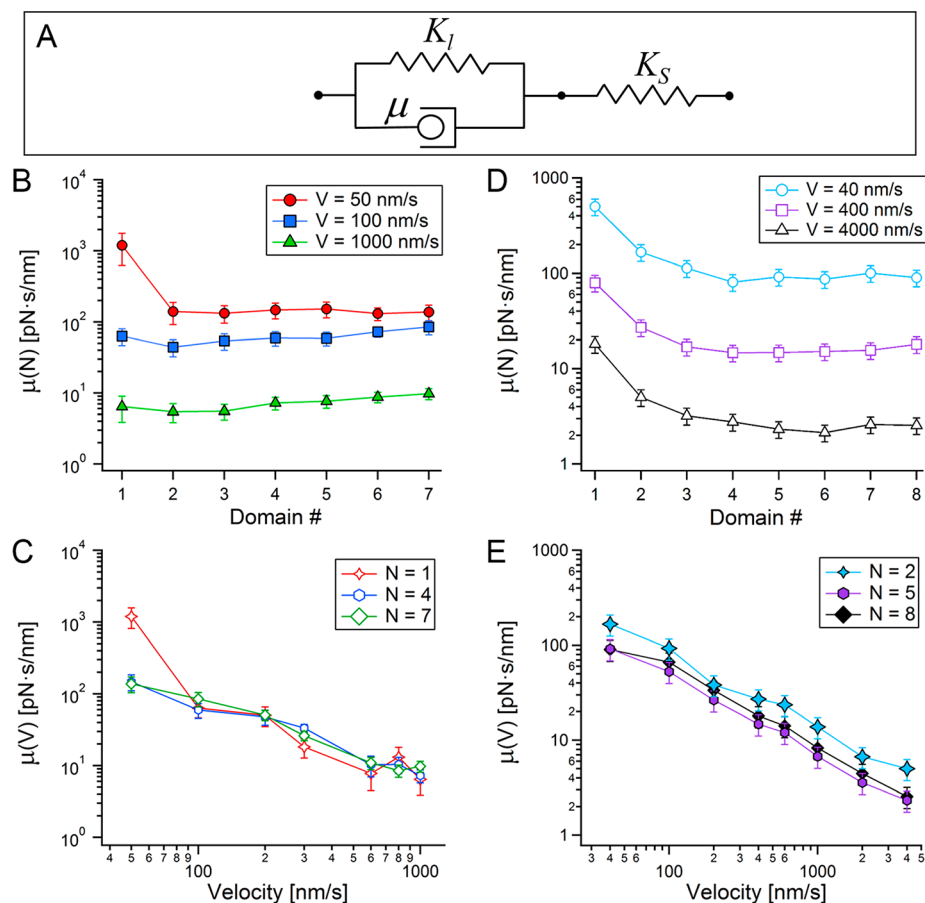
Figure 4. Viscoelastic response of the extending linker with unfolding events and pulling velocity. (A) Adaptation of the constitutive Zener model to a linker (characterized with a stiffness K_l and internal friction μ), in series with the stiffness of the probe (K_S). μ calculated with eq 5, with the experimental parameters as a function of chain length (B) and pulling velocity for three extensions (C), and with the BD parameters (D, E) respectively.

absence of an extending linker, a series of domains with a similar $\langle U_0 \rangle$ is expected to result with a proportionally similar force distributions around a mean value of $\langle F_{max} \rangle$. However, here, $\langle F_{max} \rangle$ increases as the linker chain becomes longer and softer. For this to happen, a substantial amount of the invested mechanical work $(\sim F^2/K_{eff})$ is required to achieve high stretching of the linker chain to transduce the tension on the folded molecule until it reaches the amount of stress required to overcome its $\langle U_0 \rangle$. A similar behavior is obtained with the BD simulations (Figure 5C).

An opposite trend, where the $\langle F_{max} \rangle$ grows with system stiffness, is observed for the unfolding events with similar linker length (N = const.) under increasing pulling velocities. In this situation, the faster a linker (at a given length) will be stretched, the faster the tension will propagate through it. Accordingly, the effect emerging from the presence of the linker diminishes, and the force is communicated directly to the folded domain along the polyprotein chain. The direct effect of the applied stress on folded domains (or bond rupture) is well understood within the framework of reaction-rate theory, predicting an increase of the unfolding (or rupture) forces will the applied force-rate.[44−46] This trend can be seen more explicitly in Figure 5D that presents the same properties obtained with the BD simulations. In all, the interplay of between these two mechanisms is unraveled by showing that increasing the length of the polymeric (polypeptide) linker component with each successive unfold-

ing event (at a constant pulling velocity) has an opposing effect to the one of increasing the pulling velocity (at constant length).

■ CONCLUSIONS

In this work we measured the unfolding of poly(I91) using AFM at constant pulling velocities, and performed corresponding BD simulations. By analyzing the unfolding forces, we observed a hierarchical increase of the unfolding events with the length increase of the linker with the progression of unfolding, accompanied by a decrease in the mean chain stiffness. The force-rates estimated at each pulling velocity displayed a decease with each consecutive unfolding event. Moreover, comparison of these force-rates with the conventional estimation of the force-rates as the product of the mean stiffness and pulling velocity shows that $\langle dF/dt \rangle < \langle\langle dF/dx \rangle\rangle \times V$ (or equivalently $K_{eff} \times V$). An explanation for this difference, manifested through the increase of the mean stiffness with the pulling velocity, is offered through the viscoelastic behavior of the growing linker. Finally, an interpretation of sequential unfolding in experiments performed under constant pulling velocity conditions is offered as an interplay between two underlying mechanisms: N-effect and V-effect (or dF/dt-effect).

The N-effect is an outcome of the variation in the viscoelastic properties of the linker that increases in size. The WLC phenomenological stiffness of the linker at high
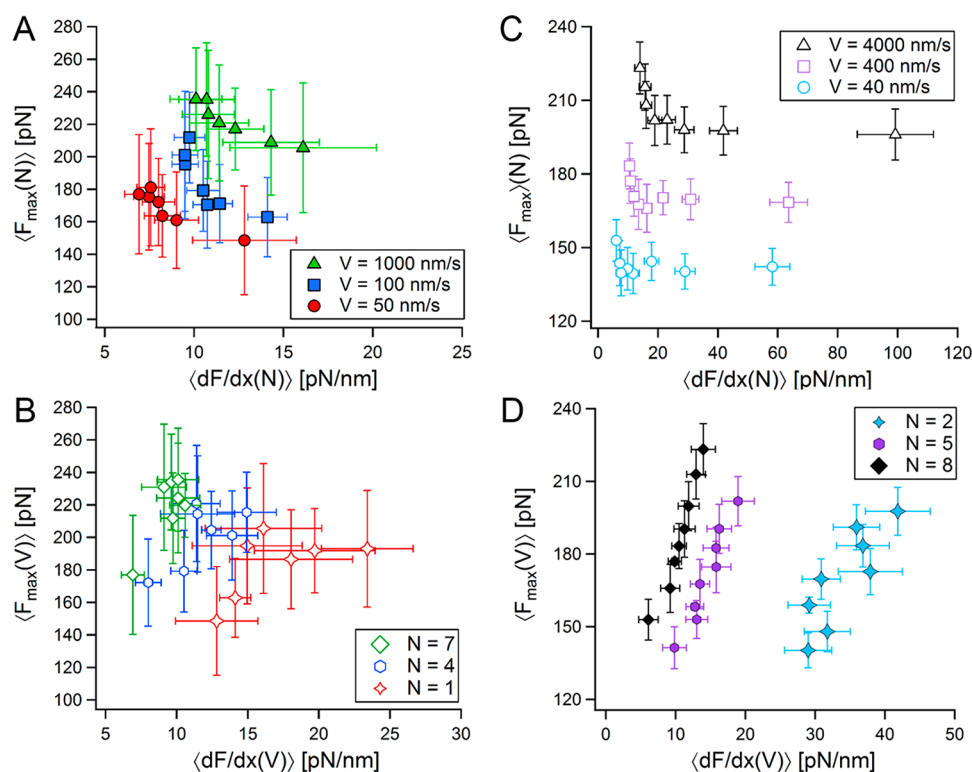
Figure 5. Measured unfolding forces as a function of their corresponding local stiffness. (A) Maximal unfolding forces vs mean chain stiffness from poly(I91) FX measurements, both as a function of domain number (chain length), at V = const. (B) Maximal unfolding forces vs mean chain stiffness from poly(I91) FX measurements, both as a function of pulling velocity, at N = const. Respectively corresponding to (A) and (B), maximal unfolding forces vs mean chain stiffness from BD simulations for V = const. (C), and N = const. (D).

stretches, $K_l(L_C, F)$,[43] given by eq 2, refers to the polymeric nature of an extending chain, at which the force serves as a cutoff value. However, here we measure a more complicated system, whose stiffness is related to the ratio between the folded and unfolded domains. If we consider the folded domains to be similar, all characterized by roughly the same $\langle U_0 \rangle$, then all domains should unfold at proportional $\langle F_{max} \rangle$, with no specific hierarchy (or N-effect). Nevertheless, in practice this is not the case. For homogeneous polyproteins (comprised from the same repeating domain), the unfolding of the domains occurs randomly,[51] where the probability of the first domain to unfold should be similar to the probability of the fifth or eighth domain to unfold. With the consecutive unfolding of every protein in the polyprotein chain, the overall length of the polymeric linker component increases with ΔL_C increments. This softens the polyprotein with every event (or alternatively, increases its compliance, as the longer linker chain is "looser" under the same load). As the overall stiffness decreases with event number, the force required for unfolding is increased, since a larger amount of work is required to further extend the longer linker, such that the tension through it will be sufficient to overcome the protein unfolding mechanical stability (the mean unfolding forces reduce with the increase of the mean stiffness). Conversely, the V-effect (or force-rate effect) causes the mean unfolding forces to increase with the increase in the force-rate application. Increasing the pulling velocity propagates the tension faster through the various components of the polyprotein chain. This communicates the perturbation faster (the chain becomes stiffer and less viscous), and thus it is directly applied to the protein. Additional measurements and simulations performed under

the application of constant force-rate, i.e., force-ramp experiments,[45] can assist in the understanding of sequential unfolding in polyproteins, particularly since the models used to interpret forced unfolding use the force-rate as the independent variable.[44,46] To conclude, stiffness lowering with domain unfolding can provide an additional mechanism to understand mechanical viscoelasticity regulation in physiological systems wherein polyproteins are involved, as in Titin, where this property is involved in tuning its performance as a complex molecular spring.[1,2]

■ ASSOCIATED CONTENT

Ⓢ Supporting Information

The Supporting Information is available free of charge at https://pubs.acs.org/doi/10.1021/acs.macromol.0c00278.

> Details on the BD simulations, unfolding forces and stiffness from BD simulations, variations of mean unfolding forces, stiffness and force rates with pulling velocity at constant length, and Zener (standard linear solid) model for the viscoelastic description of the linker (PDF)

■ AUTHOR INFORMATION

Corresponding Author

Ronen Berkovich − *Department of Chemical Engineering and The Ilze Katz Institute for Nanoscience and Technology, Ben-Gurion University of the Negev, Beer-Sheva 8410501, Israel;* ⓞ orcid.org/0000-0002-0989-6136; Email: berkovir@bgu.ac.il

Authors

Moran Elias-Mordechai − *Department of Chemical Engineering, Ben-Gurion University of the Negev, Beer-Sheva 8410501, Israel*

Einat Chetrit − *Department of Chemical Engineering, Ben-Gurion University of the Negev, Beer-Sheva 8410501, Israel*

Complete contact information is available at:
https://pubs.acs.org/10.1021/acs.macromol.0c00278

Author Contributions

R.B. conceived and planned the study. M.E.-M. and E.C. performed the measurements. M.E.-M. and R.B. and analyzed the data and wrote the paper. All authors have given approval to the final version of the manuscript.

Notes

The authors declare no competing financial interest.

■ ABBREVIATIONS

SMFS, single molecule force spectroscopy; FX, force extension; BD, Brownian-Dynamics

■ REFERENCES

(1) Rivas-Pardo, J. A.; Eckels, E. C.; Popa, I.; Kosuri, P.; Linke, W. A.; Fernandez, J. M. Work Done by Titin Protein Folding Assists Muscle Contraction. *Cell Rep.* **2016**, *14* (6), 1339−1347.

(2) Freundt, J. K.; Linke, W. A. Titin as a Force-Generating Muscle Protein under Regulatory Control. *J. Appl. Physiol.* **2019**, *126* (5), 1474−1482.

(3) del Rio, A.; Perez-Jimenez, R.; Liu, R.; Roca-Cusachs, P.; Fernandez, J. M.; Sheetz, M. P. Stretching Single Talin Rod Molecules Activates Vinculin Binding. *Science* **2009**, *323* (5914), 638−641.

(4) Haining, A. W. M.; Lieberthal, T. J.; Hernández, A. d. R. Talin: A Mechanosensitive Molecule in Health and Disease. *FASEB J.* **2016**, *30* (6), 2073−2085.

(5) Chothia, C.; Jones, E. Y. The Molecular Structure of Cell Adhesion Molecules. *Annu. Rev. Biochem.* **1997**, *66* (1), 823−862.

(6) Boggon, T. J.; Murray, J.; Chappuis-Flament, S.; Wong, E.; Gumbiner, B. M.; Shapiro, L. C-Cadherin Ectodomain Structure and Implications for Cell Adhesion Mechanisms. *Science* **2002**, *296* (5571), 1308−1313.

(7) Le, S.; Yu, M.; Yan, J. Direct Single-Molecule Quantification Reveals Unexpectedly High Mechanical Stability of Vinculin—Talin/A-Catenin Linkages. *Sci. Adv.* **2019**, *5* (12), No. eaav2720.

(8) Schwaiger, I.; Schleicher, M.; Noegel, A. A.; Rief, M. The Folding Pathway of a Fast-Folding Immunoglobulin Domain Revealed by Single-Molecule Mechanical Experiments. *EMBO Rep.* **2005**, *6* (1), 46−51.

(9) Rief, M.; Gautel, M.; Oesterhelt, F.; Fernandez, J. M.; Gaub, H. E. Reversible Unfolding of Individual Titin Immunoglobulin Domains by Afm. *Science* **1997**, *276* (5315), 1109−1112.

(10) Carrion-Vazquez, M.; Oberhauser, A. F.; Fowler, S. B.; Marszalek, P. E.; Broedel, S. E.; Clarke, J.; Fernandez, J. M. Mechanical and Chemical Unfolding of a Single Protein: A Comparison. *Proc. Natl. Acad. Sci. U. S. A.* **1999**, *96* (7), 3694−3699.

(11) Zinober, R. C.; Brockwell, D. J.; Beddard, G. S.; Blake, A. W.; Olmsted, P. D.; Radford, S. E.; Smith, D. A. Mechanically Unfolding Proteins: The Effect of Unfolding History and the Supramolecular Scaffold. *Protein Sci.* **2002**, *11* (12), 2759−2765.

(12) Kawakami, M.; Byrne, K.; Brockwell, D. J.; Radford, S. E.; Smith, D. A. Viscoelastic Study of the Mechanical Unfolding of a Protein by Afm. *Biophys. J.* **2006**, *91* (2), L16−L18.

(13) Borgia, A.; Williams, P. M.; Clarke, J. Single-Molecule Studies of Protein Folding. *Annu. Rev. Biochem.* **2008**, *77* (1), 101−125.

(14) Chen, H.; Yuan, G.; Winardhi, R. S.; Yao, M.; Popa, I.; Fernandez, J. M.; Yan, J. Dynamics of Equilibrium Folding and Unfolding Transitions of Titin Immunoglobulin Domain under Constant Forces. *J. Am. Chem. Soc.* **2015**, *137* (10), 3540−3546.

(15) Hughes, M. L.; Dougan, L. The Physics of Pulling Polyproteins: A Review of Single Molecule Force Spectroscopy Using the Afm to Study Protein Unfolding. *Rep. Prog. Phys.* **2016**, *79* (7), 076601.

(16) Rico, F.; Gonzalez, L.; Casuso, I.; Puig-Vidal, M.; Scheuring, S. High-Speed Force Spectroscopy Unfolds Titin at the Velocity of Molecular Dynamics Simulations. *Science* **2013**, *342* (6159), 741−743.

(17) Lei, H.; He, C.; Hu, C.; Li, J.; Hu, X.; Hu, X.; Li, H. Single-Molecule Force Spectroscopy Trajectories of a Single Protein and Its Polyproteins Are Equivalent: A Direct Experimental Validation Based on a Small Protein Nug2. *Angew. Chem., Int. Ed.* **2017**, *56* (22), 6117−6121.

(18) Sumbul, F.; Marchesi, A.; Rico, F. History, Rare, and Multiple Events of Mechanical Unfolding of Repeat Proteins. *J. Chem. Phys.* **2018**, *148* (12), 123335.

(19) Tapia-Rojo, R.; Eckels, E. C.; Fernández, J. M. Ephemeral States in Protein Folding under Force Captured with a Magnetic Tweezers Design. *Proc. Natl. Acad. Sci. U. S. A.* **2019**, *116* (16), 7873−7878.

(20) Pyo, A. G. T.; Woodside, M. T. Memory Effects in Single-Molecule Force Spectroscopy Measurements of Biomolecular Folding. *Phys. Chem. Chem. Phys.* **2019**, *21* (44), 24527−24534.

(21) Evans, E.; Ritchie, K. Strength of a Weak Bond Connecting Flexible Polymer Chains. *Biophys. J.* **1999**, *76* (5), 2439−2447.

(22) Hummer, G.; Szabo, A. Kinetics from Nonequilibrium Single-Molecule Pulling Experiments. *Biophys. J.* **2003**, *85* (1), 5−15.

(23) Friedsam, C.; Wehle, A. K.; K hner, F.; Gaub, H. E. Dynamic Single-Molecule Force Spectroscopy: Bond Rupture Analysis with Variable Spacer Length. *J. Phys.: Condens. Matter* **2003**, *15* (18), S1709−S1723.

(24) Ratto, T. V.; Langry, K. C.; Rudd, R. E.; Balhorn, R. L.; Allen, M. J.; McElfresh, M. W. Force Spectroscopy of the Double-Tethered Concanavalin-a Mannose Bond. *Biophys. J.* **2004**, *86* (4), 2430−2437.

(25) Janovjak, H.; Struckmeier, J.; Muller, D. J. Hydrodynamic Effects in Fast Afm Single-Molecule Force Measurements. *Eur. Biophys. J.* **2005**, *34* (1), 91−96.

(26) Ray, C.; Brown, J. R.; Akhremitchev, B. B. Correction of Systematic Errors in Single-Molecule Force Spectroscopy with Polymeric Tethers by Atomic Force Microscopy. *J. Phys. Chem. B* **2007**, *111* (8), 1963−1974.

(27) Bura, E.; Klimov, D. K.; Barsegov, V. Analyzing Forced Unfolding of Protein Tandems by Ordered Variates, 1: Independent Unfolding Times. *Biophys. J.* **2007**, *93* (4), 1100−1115.

(28) Hyeon, C.; Thirumalai, D. Forced-Unfolding and Force-Quench Refolding of Rna Hairpins. *Biophys. J.* **2006**, *90* (10), 3410−3427.

(29) Berkovich, R.; Garcia-Manyes, S.; Klafter, J.; Urbakh, M.; Fernández, J. M. Hopping around an Entropic Barrier Created by Force. *Biochem. Biophys. Res. Commun.* **2010**, *403* (1), 133−137.

(30) Maitra, A.; Arya, G. Model Accounting for the Effects of Pulling-Device Stiffness in the Analyses of Single-Molecule Force Measurements. *Phys. Rev. Lett.* **2010**, *104* (10), 108301.

(31) Maitra, A.; Arya, G. Influence of Pulling Handles and Device Stiffness in Single-Molecule Force Spectroscopy. *Phys. Chem. Chem. Phys.* **2011**, *13* (5), 1836−1842.

(32) Yoon, G.; Na, S.; Eom, K. Loading Device Effect on Protein Unfolding Mechanics. *J. Chem. Phys.* **2012**, *137* (2), 025102.

(33) Berkovich, R.; Hermans, R. I.; Popa, I.; Stirnemann, G.; Garcia-Manyes, S.; Berne, B. J.; Fernandez, J. M. Rate Limit of Protein Elastic

Response Is Tether Dependent. *Proc. Natl. Acad. Sci. U. S. A.* **2012**, *109* (36), 14416−14421.

(34) Hinczewski, M.; Gebhardt, J. C. M.; Rief, M.; Thirumalai, D. From Mechanical Folding Trajectories to Intrinsic Energy Landscapes of Biopolymers. *Proc. Natl. Acad. Sci. U. S. A.* **2013**, *110* (12), 4500−4505.

(35) Makarov, D. E. Communication: Does Force Spectroscopy of Biomolecules Probe Their Intrinsic Dynamic Properties? *J. Chem. Phys.* **2014**, *141* (24), 241103.

(36) Cossio, P.; Hummer, G.; Szabo, A. On Artifacts in Single-Molecule Force Spectroscopy. *Proc. Natl. Acad. Sci. U. S. A.* **2015**, *112* (46), 14248−14253.

(37) Tych, K. M.; Hughes, M. L.; Bourke, J.; Taniguchi, Y.; Kawakami, M.; Brockwell, D. J.; Dougan, L. Optimizing the Calculation of Energy Landscape Parameters from Single-Molecule Protein Unfolding Experiments. *Phys. Rev. E* **2015**, *91* (1), 012710.

(38) Arya, G. Models for Recovering the Energy Landscape of Conformational Transitions from Single-Molecule Pulling Experiments. *Mol. Simul.* **2016**, *42* (13), 1102−1115.

(39) De Sancho, D.; Schönfelder, J.; Best, R. B.; Perez-Jimenez, R.; Muñoz, V. Instrumental Effects in the Dynamics of an Ultrafast Folding Protein under Mechanical Force. *J. Phys. Chem. B* **2018**, *122* (49), 11147−11154.

(40) Chetrit, E.; Meroz, Y.; Klausner, Z.; Berkovich, R. Correlations within Polyprotein Forced Unfolding Dwell-Times Introduce Sequential Dependency. *J. Struct. Biol.* **2020**, 107495.

(41) Brockwell, D. J.; Beddard, G. S.; Clarkson, J.; Zinober, R. C.; Blake, A. W.; Trinick, J.; Olmsted, P. D.; Smith, D. A.; Radford, S. E. The Effect of Core Destabilization on the Mechanical Resistance of I27. *Biophys. J.* **2002**, *83* (1), 458−472.

(42) Best, R. B.; Brockwell, D. J.; Toca-Herrera, J. L.; Blake, A. W.; Smith, D. A.; Radford, S. E.; Clarke, J. Force Mode Atomic Force Microscopy as a Tool for Protein Folding Studies. *Anal. Chim. Acta* **2003**, *479* (1), 87−105.

(43) Khatri, B. S.; Byrne, K.; Kawakami, M.; Brockwell, D. J.; Smith, D. A.; Radford, S. E.; McLeish, T. C. B. Internal Friction of Single Polypeptide Chains at High Stretch. *Faraday Discuss.* **2008**, *139* (0), 35−51.

(44) Evans, E.; Ritchie, K. Dynamic Strength of Molecular Adhesion Bonds. *Biophys. J.* **1997**, *72* (4), 1541−1555.

(45) Schlierf, M.; Li, H.; Fernandez, J. M. The Unfolding Kinetics of Ubiquitin Captured with Single-Molecule Force-Clamp Techniques. *Proc. Natl. Acad. Sci. U. S. A.* **2004**, *101* (19), 7299−7304.

(46) Dudko, O. K.; Hummer, G.; Szabo, A. Intrinsic Rates and Activation Free Energies from Single-Molecule Pulling Experiments. *Phys. Rev. Lett.* **2006**, *96* (10), 108101.

(47) Nadler, H.; Shaulov, L.; Blitsman, Y.; Mordechai, M.; Jopp, J.; Sal-Man, N.; Berkovich, R. Deciphering the Mechanical Properties of Type Iii Secretion System Espa Protein by Single Molecule Force Spectroscopy. *Langmuir* **2018**, *34* (21), 6261−6270.

(48) Bustamante, C.; Marko, J.; Siggia, E.; Smith, S. Entropic Elasticity of Lambda-Phage DNA. *Science* **1994**, *265* (5178), 1599−1600.

(49) Marko, J. F.; Siggia, E. D. Stretching DNA. *Macromolecules* **1995**, *28* (26), 8759−8770.

(50) Hutter, J. L.; Bechhoefer, J. Calibration of Atomic-Force Microscope Tips. *Rev. Sci. Instrum.* **1993**, *64* (7), 1868−1873.

(51) Hoffmann, T.; Dougan, L. Single Molecule Force Spectroscopy Using Polyproteins. *Chem. Soc. Rev.* **2012**, *41* (14), 4781−4796.

(52) Fugmann, S.; Sokolov, I. M. Scaling of the Rupture Dynamics of Polymer Chains Pulled at One End at a Constant Rate. *Phys. Rev. E* **2009**, *79* (2), 021803.

(53) Severino, A.; Monge, A. M.; Rissone, P.; Ritort, F. Efficient Methods for Determining Folding Free Energies in Single-Molecule Pulling Experiments. *J. Stat. Mech.: Theory Exp.* **2019**, *2019* (12), 124001.

(54) Dobrynin, A. V.; Carrillo, J.-M. Y.; Rubinstein, M. Chains Are More Flexible under Tension. *Macromolecules* **2010**, *43* (21), 9181−9190.

(55) Zener, C. *Elasticity and Anelasticity of Metals*; University of Chicago Press: Chicago, IL, 1948.

(56) Lee, N.-K.; Thirumalai, D. Pulling-Speed-Dependent Force-Extension Profiles for Semiflexible Chains. *Biophys. J.* **2004**, *86* (5), 2641−2649.

(57) Doi, M.; Edwards, S. F. *The Theory of Polymer Dynamics*; Oxford University Press, 1988; Vol. 73.

(58) Zimm, B. H. Dynamics of Polymer Molecules in Dilute Solution: Viscoelasticity, Flow Birefringence and Dielectric Loss. *J. Chem. Phys.* **1956**, *24* (2), 269−278.

(59) Happel, J.; Brenner, H. *Low Reynolds Number Hydrodynamics: With Special Applications to Particulate Media*; Springer: The Netherlands, 1983; p 553.